

A model-driven approach for a new generation of adaptive libraries

Marco Cianfriglia*
Department of Mathematics
Rome Tre University, Italy
cianfriglia@mat.uniroma3.it

Flavio Vella
Dividiti
Cambridge, UK
flavio@dividiti.com

Cedric Nugteren
Tom Tom
Amsterdam, Netherlands
mail@cedricnugteren.nl

Anton Lokhmotov
Dividiti
Cambridge, UK
anton@dividiti.com

Grigori Fursin
Dividiti and cTuning foundation
Paris, France
grigori.fursin@ctuning.org

Abstract

Efficient high-performance libraries often expose multiple tunable parameters to provide highly optimized routines. These can range from simple loop unroll factors or vector sizes all the way to algorithmic changes, given that some implementations can be more suitable for certain devices by exploiting hardware characteristics such as local memories and vector units. Traditionally, such parameters and algorithmic choices are tuned and then hard-coded for a specific architecture and for certain characteristics of the inputs. However, emerging applications are often data-driven, thus traditional approaches are not effective across the wide range of inputs and architectures used in practice. In this paper we present a new adaptive framework for data-driven applications which uses a predictive model to select the optimal algorithmic parameters by training with synthetic and real datasets. We demonstrate the effectiveness on a BLAS library and specifically on its matrix multiplication routine. We present experimental results for two GPU architectures, and show significant performance gains of up to 3x (on a high-end NVIDIA Pascal GPU) and 2.5x (on an embedded ARM Mali GPU) when compared to a traditionally optimized library.

ACM Reference Format:

Marco Cianfriglia, Flavio Vella, Cedric Nugteren, Anton Lokhmotov, and Grigori Fursin. 2018. A model-driven approach for a new generation of adaptive libraries. In *Proceedings of ACM Conference, Washington, DC, USA, July 2017 (Conference'17)*, 14 pages.

*Most of the work was performed while the author was an intern at Dividiti.

Permission to make digital or hard copies of all or part of this work for personal or classroom use is granted without fee provided that copies are not made or distributed for profit or commercial advantage and that copies bear this notice and the full citation on the first page. Copyrights for components of this work owned by others than ACM must be honored. Abstracting with credit is permitted. To copy otherwise, or republish, to post on servers or to redistribute to lists, requires prior specific permission and/or a fee. Request permissions from permissions@acm.org.

Conference'17, July 2017, Washington, DC, USA

© 2018 Association for Computing Machinery.

ACM ISBN 978-x-xxxx-xxxx-x/YY/MM... \$15.00

<https://doi.org/10.1145/nnnnnnn.nnnnnnn>

<https://doi.org/10.1145/nnnnnnn.nnnnnnn>

1 Motivation

Scientific HPC applications are built around monolithic parallel routines that are often customized for a specific target architecture. With the advent of big-data and data-driven applications such as deep learning, graph analytics or image recognition, the traditional library design loses performance portability mainly due to the unpredictable size and structure of the data. For example, in graph processing, the computation is dictated by vertices and edges (entities and relations); therefore, it might be hard to identify an optimal parallel strategy (i.e., data-thread mapping or partitioning) a priori [6, 31]. Matrix multiplication represents another notable example where it is quite hard to determine the specific optimizations required for given input dimensions. Due to the ubiquity of matrix multiplications in many scientific applications, Basic Linear Algebra Subprograms (BLAS) and, in particular, the general matrix multiplication (GEMM) routine are the main target of optimizations. Several BLAS implementations provide fast performance on a target architecture by assuming a fixed data size or structure (i.e., square matrices) [25, 40, 51]. However, the matrices involved in the training of deep neural networks, for example, expose different sizes and usually rectangular shapes [37]. As a consequence, it is hard to find a good optimization which takes into account the wide range of data sizes involved. In practice, most BLAS libraries often provide several GEMM implementations for specific input characteristics. Such user-transparent implementations are selected by naive heuristics based on customized decision rules. However, such solutions suffer from *over-fitting* and poor performance on average.

With the wide variety of parallel architectures available on the market ranging from traditional parallel processors to accelerators (GPUs, FPGAs) and system on chips (SoCs), several standards have been established to enable portability for heterogeneous architectures such as OpenCL [45] and

OpenACC [52]. However, developing generic and performance portable code has become extremely challenging, especially from an algorithmic point of view. Here, parametric implementations and auto-tuning techniques have partially mitigated the performance portability problem by adapting the underlying memory hierarchies and/or data thread mapping to a specific architecture. Within this context, a plethora of hardware-oblivious solutions have been developed [19, 22, 38, 48].

This paper aims to offer a new prospective on adaptive libraries and performance portability to start addressing the problem of data-aware and architecture-aware software. Focusing on GPU architectures and the GEMM routine as a use case, we present a new framework based on a predictive model to select the optimal algorithm and tuning parameters to improve performance of data-driven applications.

The contributions of the paper are summarized as follows:

- we adopt a machine learning based methodology to design adaptive libraries to achieve performance portability across different datasets and hardware;
- we analyze several configurations of *decision trees*, one of the simplest univariate supervised classifiers. This is used to select an optimized implementation by predicting the algorithm and tuning parameters;
- we describe three different approaches to generate training dataset to learn predictive models;
- we validate our study by providing exhaustive experimental results where we also evaluate the performance of the predictive models in terms of the accuracy and run-time overhead;
- we integrate our solution in an OpenCL BLAS library, CLBlast [38], resulting in speed-ups of up to 3x and 2.5x for a high-end NVIDIA GPU architecture and an embedded ARM Mali GPU respectively;

The remainder of this paper is organized as follows. Section 2 provides the background. Section 3 describes our methodology and framework. Section 4 considers GEMM as a use case. Section 5 presents our exhaustive experimental evaluation. Section 6 discusses related work. Finally, Section 7 summarizes the contributions of this work and outlines its future directions.

2 Background

In this section, we provide the notation and basic concepts used in the paper. We describe the fundamentals of the decision trees classifier 2.1, the generic matrix-matrix multiplication (GEMM) routine 2.2 and CLBlast library 2.3.

2.1 Decision Tree Classifier

Decision trees is a non-parametric supervised machine learning method used for classification and regression [21, 44]. The aim is to create a model that predicts the value of a target

variable by learning simple decision rules inferred from the data features.

Decision trees have several advantages:

- most operations on a decision tree are logarithmic in the number of data points used to train the tree;
- they follow a “white box model” which is simple to understand and to interpret (unlike for example a neural network model which is more difficult to interpret);
- models can be easily translated as if-then-else statements.

Decision trees also exhibit some disadvantages:

- a decision tree might create over-complex tree that do not properly generalize the data (over-fitting);
- small variations in the data might result in a completely different tree being generated (data perturbation);
- from a complexity point of view, the problem of learning an optimal decision tree is known to be NP-complete. Consequently, practical algorithms cannot guarantee to return the globally optimal decision tree (low accuracy).

We use the scikit-learn library to build and analyze decision trees [41]. This library provides several parameters in order to define different split criteria (e.g. the maximum height of tree), the minimum number of samples required to split of an internal node, and other metrics (e.g., Gini impurity) on top of an optimized version of the CART algorithm [7].

2.2 Generic Matrix Multiplication

Matrix-multiplication is one of the key components of traditional scientific applications, but also of deep learning and other machine learning algorithms.

$$C = \alpha \cdot A \cdot B + \beta \cdot C \quad \text{s.t.} \quad A \in \mathbb{C}^{M \times K}, B \in \mathbb{C}^{K \times N}, C \in \mathbb{C}^{M \times N} \quad (1)$$

where A and B are the input matrices, C is the output and α and β are constants. The operands A and B can be optionally transposed. In general, a matrix multiplication is represented in terms of size by the tuple (M, N, K) describing the sizes of the matrices involved. The complexity is $O(M \cdot N \cdot K)$ [20]. A naive algorithm sequentially calculates each element of C by using three nested loops. However, in practice, fast computation can be achieved by maximizing data-reuse. In general, parameters, such as tiling, threads organization and scheduling can influence the performance [33]. For example, for a specific target architecture different values of tile sizes strongly impact data-reuse in local memories. Tuners explore huge search space of such parameters in order to find the best performance for a specific input size and architecture. Notable solutions and techniques about BLAS libraries and auto-tuning are reported in Section 6.

2.3 CLBlast Library

CLBlast is a modern, lightweight, fast and tunable OpenCL BLAS library written in C++11 [38]. It is designed to leverage the full performance potential of a wide variety of OpenCL devices from different vendors, including desktop and laptop GPUs, embedded GPUs, and other accelerators. The library implements BLAS routines: basic linear algebra subprograms operating on vectors and matrices. Specifically to GEMM, CLBlast provides two kernels: a “direct” kernel covering all GEMM use-cases, and an “indirect” kernel making several assumptions about the layout and sizes of the matrices. The “indirect” kernel cannot be used on its own and requires several helper kernels to pad and/or transpose matrices to meet these assumptions. Thus, there is a performance trade-off between running the more generic “direct” kernel versus the specialized “indirect” kernel ($O(n^3)$) plus several helper kernels ($O(n^2)$). Furthermore, at a kernel level, there are many

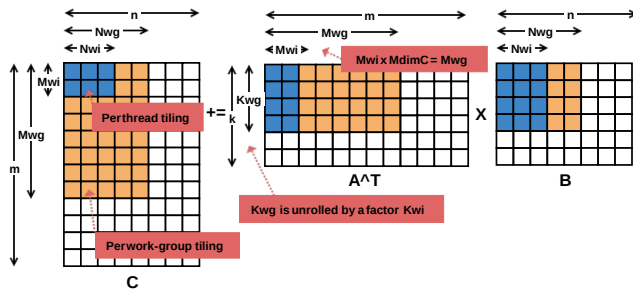


Figure 1. GEMM in CLBlast. The blue area indicates work done by a single thread, the orange area indicates work done per OpenCL work-group. Image taken from [38].

tunable parameters, 6 of which are illustrated in Figure 1. The parameters define for example the work-group sizes in 2 dimensions (M_{wg}, N_{wg}), 2D register tiling (M_{wi}, N_{wi}), vector widths of both inputs, loop unroll factors (K_{wi}), and how to use the local memories and caches. In total the search space for a GEMM kernel can easily grow to a hundred thousand realistic combinations. For more details we refer to the CLBlast and CLTune papers [38, 39].

3 Methodology and framework

In this section, we introduce a methodology and framework for generating a model-driven optimisation for input-aware adaptive libraries. The idea is to learn a model based on the inputs characteristics of a specific problem. For this purpose, we identify three desirable characteristics of the framework.

First, we should be able to select the best solution (algorithm and/or implementation and/or configuration) among multiple possible choices according to an objective function. Formally, let A be a finite set of solutions of a particular problem (e.g. matrix multiplication, graph traversal). Let $f_a : I \rightarrow \mathbb{R}$ be an objective function (e.g. floating point

operations per second (FLOPS) or traversed edges per second (TEPS)), where I is multidimensional input domain for A . For example, I can represent the set of all triples (M, N, K) which describe the GEMM operands. The goal is maximizing $\bar{a} = \arg \max_a f_a(i)$ for each $i \in I$.

Second, we should be able to build a predictive model starting from the training dataset \bar{A} consisting of all, or representative, optimal solutions \bar{a} .

Third, we should be able to generate code implementing the model. Furthermore, the generated implementation should satisfy the following requirements:

1. **correctness and soundness:** the model should be able to manage the same input domain of the original library;
2. **cost-effectiveness:** the generated code should have negligible overhead. In fact, the cost of selecting the best routine must be lower than the improvement. Formally, $f_{\bar{a}}(i) + c_{\bar{a}} < f_a(i)$ where $c_{\bar{a}}$ is the cost to select \bar{a} .

Framework design and workflow

Logically, the framework is composed of two separate phases:

1. during the off-line phase, we create a training dataset, build a predictive model from this dataset and integrate the model into the target library;
2. during the on-line phase, we use the learned model integrated into the library.

Decoupling the computationally expensive off-line phase from the on-line phase means that we can use different training datasets, as well as machine learning techniques for building models. Also, there is no need to package the machine learning framework with the target library. In our implementation, for example, a decision tree is represented by a complex if-then-else statement.

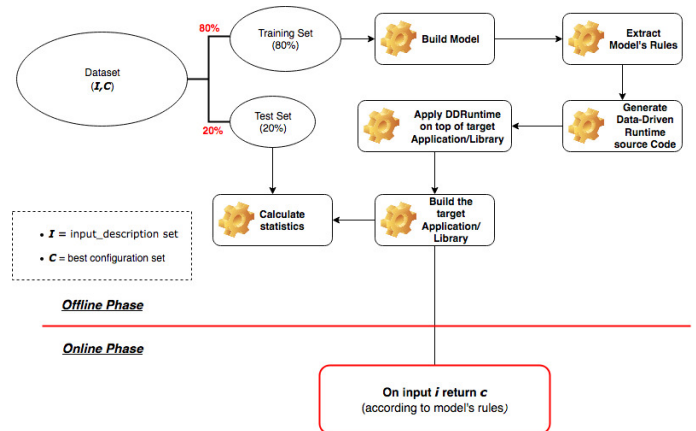


Figure 2. An overview of the proposed framework, showing the separation between the off-line (training) and on-line (deployment) phases.

Datasets

We define a dataset D as a collection of pairs (I, C) where I is the input description and C is the corresponding class description. The input description I contains information about the size (e.g. the triple (M, N, K) for GEMM), the structure (e.g. the density), and any additional information or metrics that can characterize the input (e.g. the data layout). The class description C represents the best algorithm/implementation/configuration for a given input according to the objective function. Roughly speaking, the dataset is a collection of benchmarking results over a specific set of input characteristics and a given metrics. For example, for GEMM, the metrics are usually FLOPS or FLOPS per Watt, while C is simply the best implementation/configuration for the given metrics.

Several strategies can be used for generating the dataset:

1. **synthetic**: I is generated according to a specific rule;
2. **real-world**: I is collected from real workloads;
3. **hybrid**: I is a mix of synthetic and real-world instances.

For example, for GEMM, a synthetic dataset can be generated by processing all triples (M, N, K) for which M , N , and K are all the powers of two within a domain; a real-world dataset can be collected by profiling the operands involved in a specific application such as a deep neural network (e.g. see DeepBench [37]). For graph traversal problems, a synthetic dataset can be generated from R-MAT graphs [8], while a real-world dataset can be collected from graph applications (see the SNAP dataset [28]).

A dataset D is usually divided into two disjoint subsets X and Y such that $D = \{X\} \cup \{Y\}$ via random sampling. The subsets X and Y , namely the *training dataset* and the *test dataset*, can contain for example 80% and 20% of D respectively [21].

The quality of the dataset plays a central role in the learning phase and strongly depends on the real use-case (see the next section).

Model and code generation

Several models can be created from the same training dataset X and evaluated over the test dataset Y . To learn a model, we identify the set of *features* and *labels* (or *classes*) in the training dataset; we select the input descriptions I as features and the configuration descriptions C as labels. Then, the model is learned according to the specific machine learning framework and algorithm used. Specifically, in our implementation, we use the CART algorithm to build a decision tree, but this can be replaced with any other suitable technique according to the problem at hand. Traditional machine learning techniques, such as cross validation, can also be applied in this phase. In the case of a simple decision tree, the system automatically extracts all the rules defined in internal nodes as well as the configurations represented by the leaves of tree. From the learned model, this procedure generates source code in the form of an if-then-else tree, which then gets automatically integrated into the target library.

4 A model-driven adaptation for GEMM

We present a *proof of concept* to show the effectiveness of our methodology applied to a case study. We investigate parallel matrix multiplication since it is ubiquitous in several HPC applications ranging from computational science (e.g., fluid dynamics) to deep learning and graph analytics.

4.1 Dataset

First, we define the dataset class description C according to the target library capabilities. CLBlast, in combination with CLTune, provides multiple algorithmic choices defined by tuning parameters. Table 1 summarizes CLBlast characteristics for *xgemm* and *xgemm direct* routines. According to these characteristics, the number of possible different classes for each triple (M, N, K) , which corresponds to an entry in I , is bounded by $\sum_{j=0}^{|A|} \hat{A}_j$ where \hat{A}_j is the set of the legal assignments within of the search space of the j^{th} algorithm. This distinction is necessary because some parameter combinations are invalid for a specific input or architecture. For example, a target architecture may not support too large an OpenCL work-group size or have limited local memory available.

Actually, the number of classes can be extended by increasing the search space of tunable parameters. Note that extending the search space bounds may require managing possible illegal parameters which might violate the correctness and soundness rule: each class in the dataset must be a valid configuration for each entry in I . For GEMM in CLBlast, we do not have to manage the problem of finding the best configuration ourselves. Instead, we use the existing exhaustive approach provided by the CLTune tuner [39] to find the best configurations for its two GEMM kernels (*xgemm* and *xgemm direct*) measured in terms of FLOPS. Each entry in D is a pair $((M, N, K), \bar{a})$ where \bar{a} is the best kernel represented by its tunable parameter configuration for the given (M, N, K) . From the CLBlast point of view, this means applying the tuner for the two GEMM kernels for a given (M, N, K) and recording the best solution among them. This approach is expensive when the size of I becomes significant. It is possible to trade-off quality versus time by sampling randomly from the set of tuning parameters. In this paper, however, we explore the entire search space in order to simplify the analysis during the generation of the model by avoiding perturbations on the models due to random sampling. This allows us to provide a fairer comparison among different datasets and generative model strategies.

Kernels	Tunable Parameters	Search Space Size
Gemm	14	8748
Gemm direct	9	3888

Table 1. Tuning size statistics as used for this case-study.

Second, we determine the input descriptions I of the triples (M, N, K) , and, consequently, the size and other characteristics of D . We provide one real-world dataset, and two different strategies for generating synthetic ones.

For the real-world dataset (friendly named *AntonNet*), we gather the sizes of the GEMM operands involved in popular deep neural networks: AlexNet [26], GoogLeNet [46] and SqueezeNet [24]. Specifically, we collect the sizes for the batch sizes ranging from 2 to 128 with a step of 2. This dataset consists of roughly 460 different triples, with 35% of them having $K = 1$. The other shapes are mostly rectangular.

We also generate synthetic datasets to be able to learn more generic models. In our experiments, we use two strategies that differ in terms of the distance between dataset points (M, N, K) , viewed as 3D coordinates in the Euclidean space:

1. *grid of two (go2)*: composed by (M, N, K) triples where the values range from 256 to 3840 with a step of 256. This dataset is approximately 8 times larger than *AntonNet*.
2. *power of two (po2)*: composed by (M, N, K) triples where the values are powers of 2 ranging from 64 to 2048. This dataset is less dense than *go2*.

While we can easily calculate the size of each dataset I , the number of classes C strongly depends on the architecture. For example, even if *AntonNet* is smaller than *go2*, the number of classes is 3/4 times larger for the architectures in our study (see the first four columns of Table 3 and Table 4). The main reason is that the matrices in *AntonNet* have irregular sizes and therefore require more unique configurations than the matrices in the synthetic datasets. The relation between the matrix sizes and the classes, as well as how to determine representative entries for a dataset, will be subject of further studies.

4.2 Model and code generation

A decision tree classifier usually offers multiple implementation choices in order to build a more accurate model. In our case, the parameters that we used for the training are L and H . L is the minimum number of sample per leaf required for a class to become a leaf node. This means if a class occurs one time in the dataset and $L = 2$ (or higher) that class will not become a leaf in the decision tree. Scikit also allows to set up a normalized $(0, 1)$ percentage over the total number of classes. For example with $L = 0.1$ a class to be a leaf must occur in the 10% of the dataset. A small values of L usually means the tree will overfit, whereas a large value will build more generic trees from learning the data.

H is the maximum height of the decision tree. If None, then the nodes are expanded until all the leaves are pure (all the value of the feature in the node comes from a single class) or until all leaves contain less than L samples.

To evaluate the accuracy and the performance of our approach, we trained several decision trees by tuning L and H .

Hereafter, we provide an experimental study for the evaluation of all the possible assignments of such parameters. For this case-study, we also developed a Python program to extract other features and statistics of the models that cannot be directly extrapolated from scikit-library. Examples include number of leaves or the height of the decision tree. The same program is also responsible of traversing the decision tree, extracting the rules defined into internal nodes, and all the configurations of the corresponding leaves. Consequently, the program automatically generates the corresponding C++ source code which implements the trained model in the form of an if-then-else statement. At the end of this process, the code is compiled into the library, such as CLBlast for this case-study.

5 Experimental Results

The experiments reported below aimed at investigating the following aspects:

1. the quality of the models in terms of accuracy;
2. the quality of the models in terms of the impact of misclassification;
3. the overhead of the decision tree (if-then-else statement) generated by our framework;
4. the performance of the model-driven CLBlast library against the default version tuned for a specific matrix size.

We first evaluate several models generated according to the strategies described in Section 4. Specifically, we generate and analyze the trained models by varying the maximum height and the minimum number of samples per leaf. The possible assignments of the height $H = \{1, 2, 4, 8, Max\}$, where *Max* means that there are not restriction on the height of the tree. The set of the possible assignments of the minimum number of samples per leaf is $L = \{1, 2, 4, 0.1, 0.2, 0.4, 0.5\}$.

Concerning the comparison among CLBlast versions, we refer to *peak* when we report the best performance of CLBlast tuned for a generic matrix (M, N, K) . This operation requires to run the tuner for both gemm routines. Notice that the tuner returns the kernel time to perform the matrix multiplication only. In the case of *xgemm*, this does not include the time required to perform auxiliary kernels, thus it represents a performance upper bound of CLBlast. The peak of the tuner gives an estimation of how much the performance of a model is far away from the possible best. This information also reflects the ability of the code to adapt to the architecture for a given input size.

We refer to CLBlast *default* when we use the CLBlast with the optimal parameters for a default matrix size which corresponds to $M=N=K=1024$ for *xgemm* and $M=N=K=256$ for *xgemm direct*. In CLBlast, the mechanism for switching *xgemm direct* and *xgemm* kernel is based on a value of threshold. Such threshold takes into account the sizes of the

operands involved in the multiplication. This approach basically implements a linear cut of the space represented by the triples (M, N, K) by assigning one gemm implementation and its own configuration. Finally, we refer to *model*, when we report the performance of our model-driven CLBLast version. To automatize the workflow of our framework, we used Collective Knowledge technology [18] for generating the datasets, learning the models and evaluating their performance.

5.1 Hardware setup

We focused on two different GPU architectures: a high-end NVIDIA Tesla P100 based on the Pascal architecture and an embedded ARM Mali-T860 based on the Midgard architecture. In Table 2, we report a summary of the main characteristics of both architectures. For the ARM GPU, we did not generate the *go2* dataset due to the limited amount of hours available.

Device name	Nvidia P100	ARM Mali-T860
Market segment	Server	System on Chip
Micro-architecture	Pascal	Midgard 4th gen
Number of available cores	3584 CUDA cores (GP100)	4 Mali cores
Boost frequency	1353 MHz	2000 MHz
Processing power	9.7 TFLOPS	23.8 GFLOPS
Memory available	16 GB	4 GB
Memory type	HBM2	DDR3

Table 2. Nvidia P100 and ARM Mali-T860 hardware description.

5.2 Accuracy and Misclassification

To estimate the quality of the models, we calculate the accuracy by using scikit-learn. The accuracy is a standard measure for classification problems with the aim of providing a measure of the quality of a given model in terms of right predictions on the test dataset. It is defined as the ratio between the number of right prediction and the total number of instances in the test dataset. Therefore, it allows to validate and evaluate different models since the classes for each entry are known *a priori*. In our scenario, the classes are represented by the set of configurations, and implicitly by the corresponding gemm implementation as we found out through the tuner. For two different consecutive triples (i.e. $(256, 256, 256)$ and $(256, 512, 256)$) such configurations might be likely similar to each other. In some case, we noticed that the best configuration for a specific triple (M, N, K) achieves good performance for the nearest triples. In those cases, a model likely selects a configuration $C'_{m_i} \neq C^{best}_{m_i}$ that is not too far away in terms of performance from the optimum. However, from classification task prospective that represents a misclassification. For this kind of applications, accuracy does not give a good estimation of the real performance of the model since it does not take into account the impact of the misclassification. To overcome

this problem, we defined two metrics in order to measure the real performance of the models over the test dataset. The first metric is defined as the average of the ratio between the performance of a model over the peak of performance of the tuner. Likewise, the second one takes into account the performance of a model over the performance of the tuned version of CLBLast. We denote them as **DTPR** ('decision tree peak ratio') and **DTTR** ('decision tree tune ratio') respectively. **DTPR** metrics provides a more accurate estimation of the models as it is able to quantify the performance of a class also in the presence of misclassification.

5.3 Models evaluation

We start our analysis by measuring the accuracy of several models learned from our datasets by varying H and L parameters. Models should be able to predict the right class among up to 82 differ classes (see the sum per row of the columns 3 and 4 in Table 3 and Table 4). Specifically, Figure 3 shows the accuracy (y-axis) of all the models (x-axis) generated by our framework for the Nvidia P100 (Figure 3a) and the ARM Mali-T860 (Figure 3b). We first noticed that a denser and regular dataset, like *go2*, has a higher accuracy than a more sparse dataset like *po2*. Unexpectedly, on the Mali GPU, *AntonNet* shows a better accuracy. In general, we observe that the accuracy mainly depends on the distribution between gemm kernels and the number of unique configurations in the dataset (see Table 3 and Table 4). An unbalanced distribution of such configurations can be observed both *AntonNet* and *po2* on the Nvidia P100. For example, by looking at Table 3 (columns 3-4), the configurations in these datasets mainly correspond to *xgemm direct* kernel. The reason is that Nvidia P100 has enough resources to perform *xgemm direct* in the most of the cases. Thus, in this specific case, the classes corresponding to *xgemm* will be hardly represented in the model even if the model is trained with a low value of L . Contrarily, on the ARM GPU the configurations of *AntonNet* are more uniformly distributed among the gemm implementations (see Table 4). From the results we observed, H and L parameters do not impact on the accuracy significantly. As an example, Figure 3a shows the same trend for *go2*, *po2* and *AntonNet* datasets even if L parameter changes. Summarizing, the model learned from *go2* with $H = 8$ and $L = 1$ achieves the highest accuracy on the Nvidia GPU, meanwhile the model $H = 4$ and $L = 1$ trained from *AntonNet* represents the best for the ARM GPU.

Accuracy experiments indirectly shows that the accuracy decreases in the presence of an increasing unbalancing distribution of the kernels and configurations. Contrarily, **DTPR** and **DTTR** experiments indirectly provide a measure of the similarity between classes (kernel and configuration) in terms of performance: this allows measuring the impact of the misclassification. Figure 4 and Figure 5 show **DTPR** and **DTTR** values for each model (see the x-axis of the figures). Unlike the accuracy, the values of these metrics depends on the

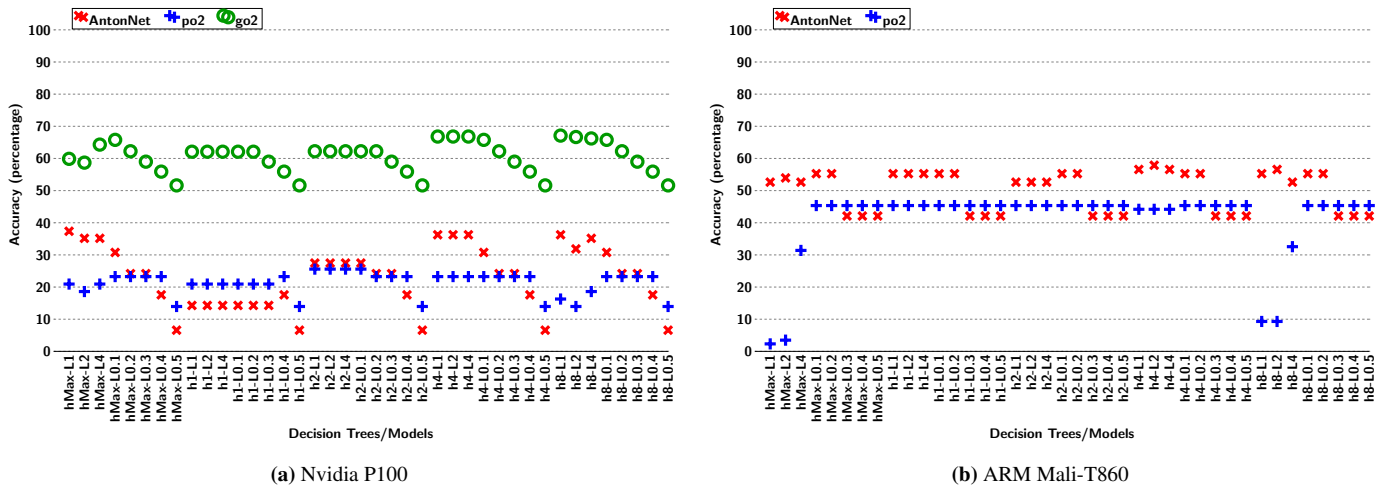


Figure 3. Accuracy evaluation of the models generated by varying H and L parameters on $go2$ (Nvidia only), $po2$ and $AntonNet$ dataset.

Dataset Name	Dataset Size	Number of Unique Config. Xgemm	Number of Unique Config. XgemmDirect	Best Decision Tree Name	Best Decision Tree accuracy	Best Decision Tree DTPR	Best Decision Tree DTTR
AntonNet	456	1	81	h4-L1	36	0.484	1.013
PowerOf2(po2)	216	2	41	hMax-L1	21	0.431	0.931
GridOf2(go2)	3375	6	22	hMax-L1	60	0.852	1.424

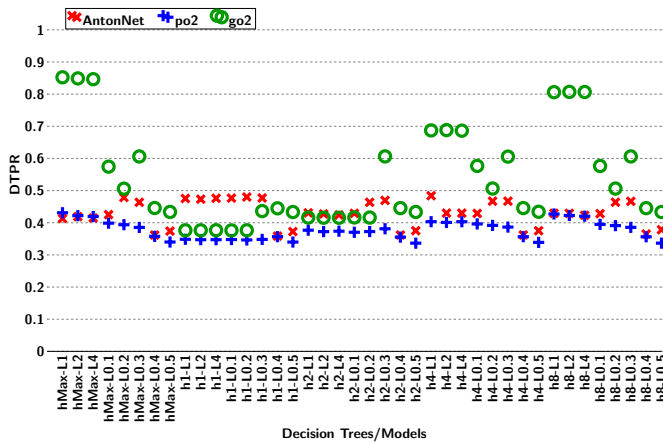
Table 3. Datasets statistics - Nvidia P100. “Best Decision Tree” refers to the model with the highest **DTTR** score. The sum (per row) of the columns 3 and 4 represents the total number of classes of the dataset.

Dataset Name	Dataset Size	Number of Unique Config. Xgemm	Number of Unique Config. XgemmDirect	Best Decision Tree Name	Best Decision Tree accuracy	Best Decision Tree DTPR	Best Decision Tree DTTR
AntonNet	456	28	35	h1-L0.1	55	0.702	1.092
PowerOf2(po2)	216	29	1	h8-L0.1	45	0.551	1.121

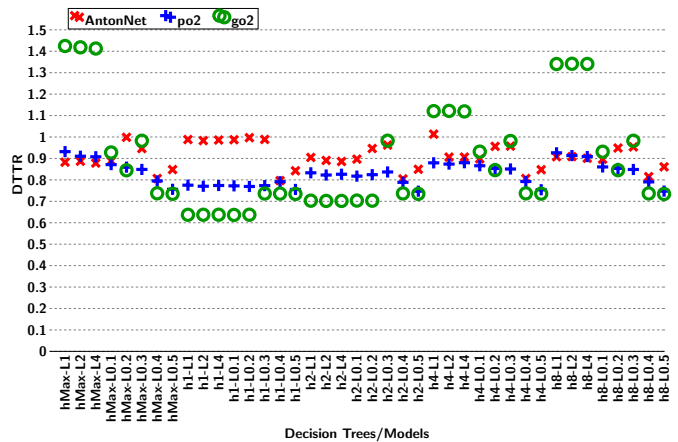
Table 4. Dataset statistics - ARM Mali-T860. “Best Decision Tree” refers to the model with the highest **DTTR** score. The sum (per row) of the columns 3 and 4 represents the total number of classes of the dataset.

choice of H and L parameters. In particular, the value of the minimum number of samples per leaf strongly influences the performance. Such parameter implicitly assigns a weight to the classes, thus such values are proportional to the number of occurrences of the class in the dataset. In detail, as for Nvidia architecture, $go2$ again shows the best performance. By analyzing Figure 4a, different models (x-axis) achieve high scores (**DTPR** > 0.7) meanwhile the impact of the misclassification of models learned from the other datasets is particular relevant. This result is also evident by analyzing **DTTR** values in Figure 4b. For the ARM architecture, the landscape is different. As a matter of fact, overfitted models (see for example the models with $L = 0.1$ in Figure 5b) mitigate the impact of the misclassification improving **DTPR** scores on $AntonNet$. On top on the results we showed, **DTTR** scores also provide a preliminary measure of the performance of the model-driven CLBlast against the standard tuned CLBlast.

From the **DTTR** results of the models trained from $po2$ and $AntonNet$ datasets, the model-driven CLBlast library shows the same performance of the traditional tuned version on the Nvidia GPU. Likewise, the **DTPR** scores give a preliminary estimation of how much the models are close to the best possible solution. Finally, just for completeness, we report in Table 5 all the statistics and metrics for all the decision trees learned from the dataset $go2$ on the Nvidia GPU. By analyzing our metrics, the best model is $hMax-L1$ even if $h8-L1$ have a higher accuracy (67%). As a consequence, an improvement of the accuracy of the decision trees does not guarantee an improvement in terms of performance. Regarding Mali GPU, we report in Table 6 the statistics of the models generated from $AntonNet$.

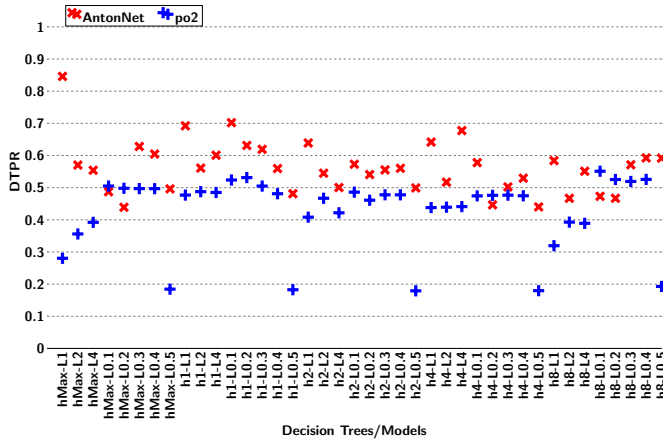


(a) Average performance ratio between the model-driven and the peak of the tuner of CLBlast (DTTPR).

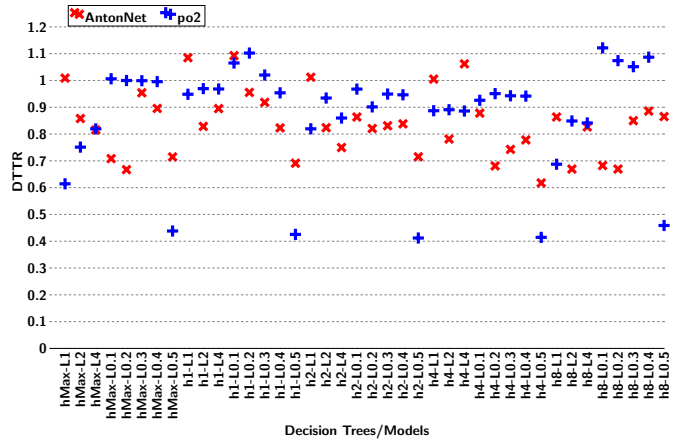


(b) Average performance ratio between the model-driven and the tuned version of CLBlast (DTTR).

Figure 4. Evaluation of the impact of misclassification of the models generated by varying H and L parameters on *go2*, *po2* and *AntonNet* dataset on Nvidia P100.



(a) Average performance ratio between the model-driven and the peak of the tuner of CLBlast (DTTPR).



(b) Average performance ratio between the model-driven and the tuned version of CLBlast (DTTR).

Figure 5. Evaluation of the impact of misclassification of the models generated by varying H and L parameters on *po2* and *AntonNet* dataset on ARM Mali-T860.

5.4 MicroBenchmark

The previous experiments showed the average performance ratio of the model-driven CLBlast against both the traditionally tuned CLBlast (v1.0), and the peak performance of the tuner over all the matrices in the test dataset randomly generated. For the evaluation of the impact of the misclassification that is important, especially when the goal is evaluating several models that are trained from very specific datasets like *AntonNet*. The metrics **DTTPR** and **DTTR** measure how a model is good

in general in terms of performance, overfitting and misclassification. Thus, our metrics are good indicators for the selection of the most promising models. However, the average of the ratio might not provide a good estimation of the real performance. For example, for specific matrices the improvement may be no relevant when the number of operations (FLOPS) are small (see for example the first triple in Figure 7b). Thus, hereafter, we show the performance in GFLOPS, of the model-driven CLBlast against the traditionally tuned CLBlast and the peak performance of the tuner over a wide range of matrices of test datasets. In Figure 6 and Figure 7, we report the

performance of the best model we found for each datasets on Nvidia and ARM architectures respectively. For Nvidia P100, the model *hMax-L1* learned from *go2* achieves very good performance in most of the points, with the maximum speed-up of 3x over the traditional tuned CLBlast (Figure 6a). *DTTR* shows an improvement of 1.42x on average. This is mainly due to the modest improvement on the matrices close to the default size used in the traditional tuned version. On the contrary, looking at the results of the model learned from a more sparse dataset, the model-driven approach does not guarantee satisfactory performance on average even if in some case it is able to achieve good speed-ups as shown in Figure 6b. On the Mali-T860, Figure 7a surprisingly shows significant speed-ups (up to 2.5x) for several matrices even if **DDTR** states a small improvement on the average (1.12x). For both the architectures, the models learned from *AntonNet* dataset show unsatisfactory performance even if the models have good accuracy on the Mali GPU. One reason is that the decision tree classifier is not able to learn a good model (in term of performance) from a very specific datasets as *AntonNet*. Secondly, the misclassification represent an important issue in this case: for the matrices in the dataset, the configurations learned are very specific and different from each other. This means that the wrong configuration (and kernel) selected by the model usually achieves very poor performance. Third, the gap between CLBlast tuned and the peak of the tuner is not significant (see Figure 7b). This means that both the tuner and gemm implementations do not achieve good performance *per se*. Summarizing about performance, the best models found *hMax-L1* (trained from *go2*) for Nvidia and *h8-L0.1* (trained from *po2*) for ARM outperform the tuned CLBlast as shown in Figure 6a and Figure 7a. Thus, that models should be used in practice in real applications. We finally conclude the section by showing the cost to traverse the decision tree and thus quantify the overhead of the code generated by our framework. We analyzed *hMax-L1* model on *go2* (which has 1200 leaves and depth equal to 19) over all the matrices in the test dataset. The corresponding if-then-else statement introduces less than 2% of overhead on small matrices by selecting the deepest leaf. It definitively decreases as the size of the matrices grows. On average, the overhead impacts less than 1% on performance. We observed a similar trend on the ARM based architecture.

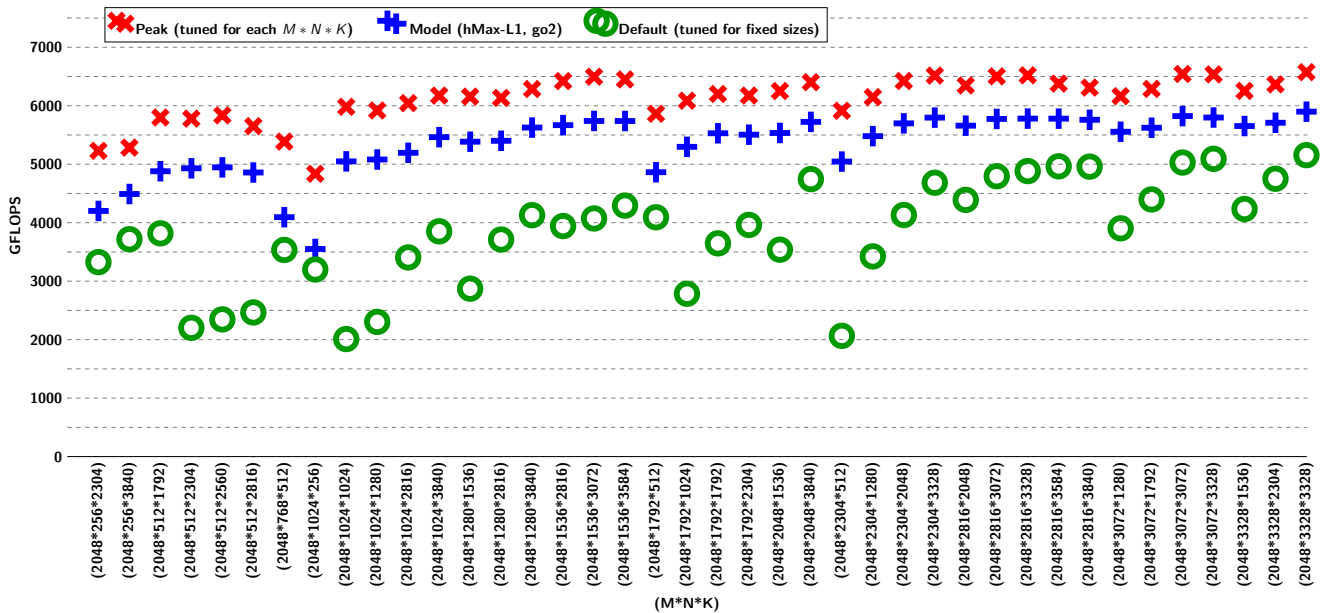
6 Related Work

There are several papers and notable results that have inspired our works. Some of them have been focused on input- and hardware-aware methodologies, meanwhile others target BLAS optimization specifically. More recently, with the pandemic adoption of the machine learning [1, 21, 36], model-driven approaches come out. Auto-tuning and input aware techniques [13, 16] are recently used to address the problem

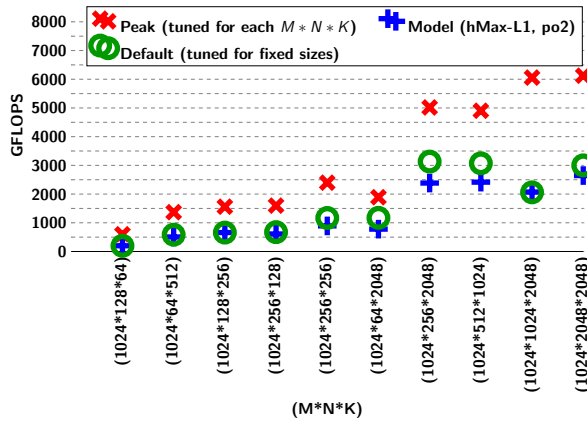
of performance portability on different data-driven applications [11, 23, 32]. An interesting approach extends such techniques in the presence of multiple algorithmic choice [42]. However, their on-line solution is suitable when a specific routine is called multiple times. As for hardware-oblivious approaches, the Nitro framework provides cross-architecture performance portability by building a model on a target architecture from training on different source architectures [35]. Specifically to BLAS, several optimized linear algebra and BLAS libraries have been released [2, 9, 50, 53]. Some of them have been designed for accelerators [14, 38, 43] or for specific GPU architectures only [40]. Several works have previously published auto-tuning and optimization approaches to accelerate GEMM [27, 30, 34]. The problem of the exploration of huge search space of tunable parameters has been partially mitigated by the use of meta-heuristics optimization approaches [39, 49] and machine learning techniques [16, 47]. The formers are able to predict parameters by starting from the exploration of a small search space [4, 12, 17]. From industrial perspective, vendors libraries (e.g., MKL, cuBLAS and ARM Compute Library) still apply manual heuristics in order to select at runtime highly-optimized code for specific inputs. Contrarily to those solutions, recently model-driven solutions have been adopted for selecting the best numerical method to solve the linear advection equation [3] and optimizing sparse CP decomposition [29]. Others investigated machine learning techniques to accelerate sparse linear algebra operations [10, 15, 54]. Tillet et al., developed ISAAC, which exploits a multi-layer perceptron (MLP) to generate high optimized parametric-code in the training step, such that at run-time, the library infers the best parameters for the specific input [47]. However, since it generates assembly code, it is not able to run on different architectures like ARM. Contrarily to the existing works, our solution is general since it can be applied to different architectures and problems. Especially for the architecture perspective, we do not need the exposure of the instruction set as ISAAC [47] requires. This also makes our solution robust since it is not affected by architectural changes.

7 Conclusion

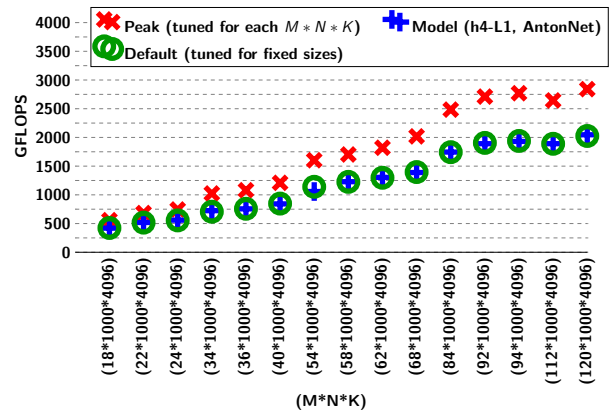
When designing high performance applications, a key problem is how to select the optimal algorithm/implementation/-configuration for a given combination of data types, data sizes, system capabilities, etc. In this paper, we presented a machine learning based approach to building highly-optimized adaptive libraries for data-driven applications. We analyzed a simple white-box supervised classifier to build a predictive model for GEMM on GPUs. We analyzed in depth the performance of several models trained from different datasets and generated by tuning different parameters. While decision trees did not achieve particularly high accuracy, we still observed significant performance improvements (up to 3x)



(a) Dataset: go2. Model: hMax-L1.



(b) Dataset: po2. Model: hMax-L1.



(c) Dataset: AntonNet. Model: h4-L1.

Figure 6. Performance evaluation of model-driven CLBlast vs CLBlast traditionally tuned on Nvidia P100.

compared to the traditional, non-adaptive approach: in practice, the impact of mispredictions is mitigated when the model is generated from a dense dataset, even when using just a few features. We validated this approach with a production-quality BLAS OpenCL library on two very different GPU architectures. We are planning to release our source code and the datasets as customizable and reusable Collective Knowledge components.

We are extending this work in several directions. First, we are investigating advanced ML techniques to generate more effective models, especially when the training datasets are small and potentially specific (like AntonNet). Second, we

looking into how to generate more compact but still representative training sets. This aspect is particularly crucial for embedded architectures where generating the training set is expensive (e.g., it took 7 days to create po2 for the Mali GPU). We believe in a collaborative/community-driven approach for collecting and analyzing datasets, building predictive models, etc. [18].

Finally, we are studying more complex problems such as graph analytics, where it is hard to predict the computation due to many possible choices for data structures (e.g. CSR or COO) [54], data-thread mapping strategies (vertex or edge parallelism) and algorithms (e.g. top-down or bottom-up [5]).

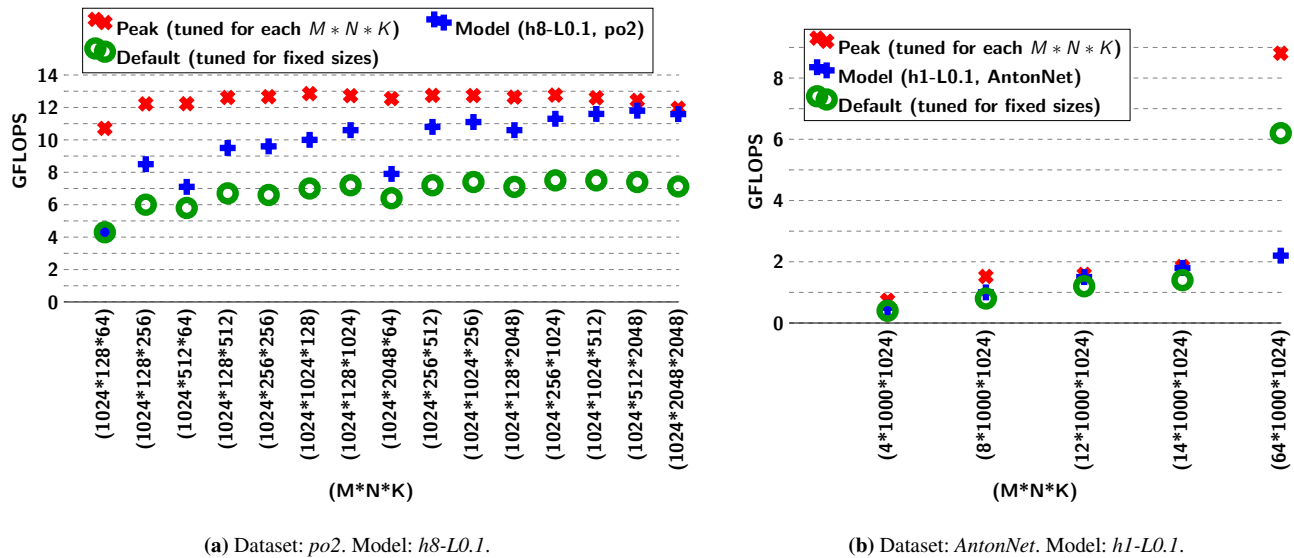


Figure 7. Performance evaluation of model-driven CLBlast vs CLBlast traditionally tuned on ARM Mali-T860.

8 Acknowledgements

Marco Cianfriglia was supported by HiPEAC projec “Industrial PhD Internship 2016”. The HiPEAC project has received funding from the European Union’s Horizon 2020 research and innovation programme under grant agreement number 779656.

References

- [1] E. Alpaydin. *Introduction to machine learning*. MIT press, 2014.
- [2] E. Anderson, Z. Bai, J. Dongarra, A. Greenbaum, A. McKenney, J. Du Croz, S. Hammerling, J. Demmel, C. Bischof, and D. Sorensen. Lapack: A portable linear algebra library for high-performance computers. In *Proceedings of the 1990 ACM/IEEE conference on Supercomputing*, pages 2–11. IEEE Computer Society Press, 1990.
- [3] A. Arteaga, O. Fuhrer, T. Hoefler, and T. Schulthess. Model-driven choice of numerical methods for the solution of the linear advection equation. *Procedia Computer Science*, 108:1542–1551, 2017.
- [4] J. Bergstra, N. Pinto, and D. Cox. Machine learning for predictive auto-tuning with boosted regression trees. In *2012 Innovative Parallel Computing (InPar)*, pages 1–9, May 2012.
- [5] M. Bernaschi, M. Bisson, E. Mastrorostefano, and F. Vella. Multilevel parallelism for the exploration of large-scale graphs. *IEEE Transactions on Multi-Scale Computing Systems*, PP(99):1–1, 2018.
- [6] M. Bernaschi, G. Carbone, and F. Vella. Scalable betweenness centrality on multi-gpu systems. In *Proceedings of the ACM International Conference on Computing Frontiers*, pages 29–36. ACM, 2016.
- [7] L. Breiman, J. Friedman, C. J. Stone, and R. A. Olshen. *Classification and regression trees*. CRC press, 1984.
- [8] D. Chakrabarti, Y. Zhan, and C. Faloutsos. R-mat: A recursive model for graph mining. In *Proceedings of the 2004 SIAM International Conference on Data Mining*, pages 442–446. SIAM, 2004.
- [9] J. Choi, J. J. Dongarra, R. Pozo, and D. W. Walker. Scalapack: A scalable linear algebra library for distributed memory concurrent computers. In *Frontiers of Massively Parallel Computation, 1992., Fourth Symposium on the*, pages 120–127. IEEE, 1992.
- [10] J. W. Choi, A. Singh, and R. W. Vuduc. Model-driven autotuning of sparse matrix-vector multiply on gpus. In *Proceedings of the 15th ACM SIGPLAN Symposium on Principles and Practice of Parallel Programming*, PPOPP ’10, pages 115–126, New York, NY, USA, 2010. ACM.
- [11] B. Cosenza, J. J. Durillo, S. Ermon, and B. Juurlink. Autotuning stencil computations with structural ordinal regression learning. In *Parallel and Distributed Processing Symposium (IPDPS), 2017 IEEE International*, pages 287–296. IEEE, 2017.
- [12] B. Cosenza, J. J. Durillo, S. Ermon, and B. Juurlink. Autotuning stencil computations with structural ordinal regression learning. In *2017 IEEE International Parallel and Distributed Processing Symposium (IPDPS)*, pages 287–296, May 2017.
- [13] Y. Ding, J. Ansel, K. Veeramachaneni, X. Shen, U.-M. O’Reilly, and S. Amarasinghe. Autotuning algorithmic choice for input sensitivity. *SIGPLAN Not.*, 50(6):379–390, June 2015.
- [14] P. Du, R. Weber, P. Luszczek, S. Tomov, G. Peterson, and J. Dongarra. From cuda to opencl: Towards a performance-portable solution for multi-platform gpu programming. *Parallel Computing*, 38(8):391–407, 2012.
- [15] A. Elafrou, G. Goumas, and N. Koziris. Performance analysis and optimization of sparse matrix-vector multiplication on modern multi- and many-core processors. In *Parallel Processing (ICPP), 2017 46th International Conference on*, pages 292–301. IEEE, 2017.
- [16] T. L. Falch and A. C. Elster. Machine learning based auto-tuning for enhanced opencl performance portability. In *Parallel and Distributed Processing Symposium Workshop (IPDPSW), 2015 IEEE International*, pages 1231–1240. IEEE, 2015.
- [17] T. L. Falch and A. C. Elster. Machine learning-based auto-tuning for enhanced performance portability of opencl applications. *Concurrency and Computation: Practice and Experience*, 29(8):e4029–n/a, 2017. e4029 cpe.4029.
- [18] G. Fursin, A. Likhomotov, and E. Plowman. Collective Knowledge: Towards R&D sustainability. In *2016 Design, Automation Test in Europe Conference Exhibition (DATE)*, pages 864–869, March 2016.
- [19] V. Goyal, Y. Ishai, A. Sahai, R. Venkatesan, and A. Wadia. Founding cryptography on tamper-proof hardware tokens. In *Proceedings of*

- the 7th international conference on Theory of Cryptography, pages 308–326. Springer-Verlag, 2010.
- [20] A. Grama. *Introduction to parallel computing*. Pearson Education, 2003.
- [21] J. Han, M. Kamber, and J. Pei. *Data Mining: Concepts and Techniques*. Morgan Kaufmann Publishers Inc., San Francisco, CA, USA, 3rd edition, 2011.
- [22] M. Heimel, M. Saecker, H. Pirk, S. Manegold, and V. Markl. Hardware-oblivious parallelism for in-memory column-stores. *Proceedings of the VLDB Endowment*, 6(9):709–720, 2013.
- [23] K. Hou, W.-c. Feng, and S. Che. Auto-tuning strategies for parallelizing sparse matrix-vector (spmv) multiplication on multi-and many-core processors. In *Parallel and Distributed Processing Symposium Workshops (IPDPSW), 2017 IEEE International*, pages 713–722. IEEE, 2017.
- [24] F. N. Iandola, S. Han, M. W. Moskewicz, K. Ashraf, W. J. Dally, and K. Keutzer. Squeezenet: Alexnet-level accuracy with 50x fewer parameters and < 0.5 mb model size. *arXiv preprint arXiv:1602.07360*, 2016.
- [25] Intel. Intel math kernel library. reference manual, 2018. Santa Clara, USA. ISBN 630813-054US.
- [26] A. Krizhevsky, I. Sutskever, and G. E. Hinton. Imagenet classification with deep convolutional neural networks. In *Advances in neural information processing systems*, pages 1097–1105, 2012.
- [27] J. Lai and A. Sezenc. Performance upper bound analysis and optimization of sgemm on fermi and kepler gpus. In *Code Generation and Optimization (CGO), 2013 IEEE/ACM International Symposium on*, pages 1–10. IEEE, 2013.
- [28] J. Leskovec and A. Krevl. SNAP Datasets: Stanford large network dataset collection. <http://snap.stanford.edu/data>, June 2014.
- [29] J. Li, J. Choi, I. Perros, J. Sun, and R. Vuduc. Model-driven sparse cp decomposition for higher-order tensors. In *Parallel and Distributed Processing Symposium (IPDPS), 2017 IEEE International*, pages 1048–1057. IEEE, 2017.
- [30] Y. Li, J. Dongarra, and S. Tomov. A note on auto-tuning gemm for gpus. *Computational Science—ICCS 2009*, pages 884–892, 2009.
- [31] A. Lumsdaine, D. Gregor, B. Hendrickson, and J. Berry. Challenges in parallel graph processing. *Parallel Processing Letters*, 17(01):5–20, 2007.
- [32] A. Magni, D. Grewe, and N. Johnson. Input-aware auto-tuning for directive-based gpu programming. In *Proceedings of the 6th Workshop on General Purpose Processor Using Graphics Processing Units, GPGPU-6*, pages 66–75, New York, NY, USA, 2013. ACM.
- [33] K. Matsumoto, N. Nakasato, and S. G. Sedukhin. Implementing a code generator for fast matrix multiplication in OpenCL on the GPU. In *2012 IEEE 6th International Symposium on Embedded Multicore SoCs*, pages 198–204, Sept 2012.
- [34] K. Matsumoto, N. Nakasato, and S. G. Sedukhin. Performance tuning of matrix multiplication in opencl on different gpus and cpus. In *High Performance Computing, Networking, Storage and Analysis (SC), 2012 SC Companion:*, pages 396–405. IEEE, 2012.
- [35] S. Muralidharan, M. Shantharam, M. Hall, M. Garland, and B. Catanzaro. Nitro: A framework for adaptive code variant tuning. In *2014 IEEE 28th International Parallel and Distributed Processing Symposium*, pages 501–512, May 2014.
- [36] K. Murphy. Machine learning: a probabilistic approach. *Massachusetts Institute of Technology*, pages 1–21, 2012.
- [37] S. Narang. DeepBench. [urlhttps://github.com/baidu-research/DeepBench](https://github.com/baidu-research/DeepBench). last access 20 October 2017.
- [38] C. Nugteren. CLBlast: A Tuned OpenCL BLAS Library. *CoRR*, abs/1705.05249, 2017.
- [39] C. Nugteren and V. Codreanu. CLTune: A Generic Auto-Tuner for OpenCL Kernels. *2015 IEEE 9th International Symposium on Embedded Multicore/Many-core Systems-on-Chip (MCSoc)*, 00:195–202, 2015.
- [40] Nvidia. Cublas library. *NVIDIA Corporation, Santa Clara, California*, 15(27):31, 2008.
- [41] F. Pedregosa, G. Varoquaux, A. Gramfort, V. Michel, B. Thirion, O. Grisel, M. Blondel, P. Prettenhofer, R. Weiss, V. Dubourg, J. Vanderplas, A. Passos, D. Cournapeau, M. Brucher, M. Perrot, and E. Duchesnay. Scikit-learn: Machine learning in python. *J. Mach. Learn. Res.*, 12:2825–2830, Nov. 2011.
- [42] P. Pfaffe, M. Tillmann, S. Walter, and W. F. Tichy. Online-autotuning in the presence of algorithmic choice. In *2017 IEEE International Parallel and Distributed Processing Symposium Workshops (IPDPSW)*, pages 1379–1388, May 2017.
- [43] K. Rupp, F. Rudolf, and J. Weinbub. Viennacl-a high level linear algebra library for gpus and multi-core cpus. In *Intl. Workshop on GPUs and Scientific Applications*, pages 51–56, 2010.
- [44] S. R. Safavian and D. Landgrebe. A survey of decision tree classifier methodology. *IEEE transactions on systems, man, and cybernetics*, 21(3):660–674, 1991.
- [45] J. E. Stone, D. Gohara, and G. Shi. Opencl: A parallel programming standard for heterogeneous computing systems. *Computing in science & engineering*, 12(3):66–73, 2010.
- [46] C. Szegedy, W. Liu, Y. Jia, P. Sermanet, S. Reed, D. Anguelov, D. Erhan, V. Vanhoucke, and A. Rabinovich. Going deeper with convolutions. In *Proceedings of the IEEE conference on computer vision and pattern recognition*, pages 1–9, 2015.
- [47] P. Tillet and D. Cox. Input-aware auto-tuning of compute-bound hpc kernels. In *Proceedings of the International Conference for High Performance Computing, Networking, Storage and Analysis, SC '17*, pages 43:1–43:12, New York, NY, USA, 2017. ACM.
- [48] P. Tillet, K. Rupp, and S. Selberherr. An automatic opencl compute kernel generator for basic linear algebra operations. In *Proceedings of the 2012 Symposium on High Performance Computing, HPC '12*, pages 4:1–4:2, San Diego, CA, USA, 2012. Society for Computer Simulation International.
- [49] B. Van Werkhoven, J. Maassen, H. E. Bal, and F. J. Seinstra. Optimizing Convolution Operations on GPUs Using Adaptive Tiling. *Future Gener. Comput. Syst.*, 30:14–26, Jan. 2014.
- [50] R. C. Whaley and J. J. Dongarra. Automatically tuned linear algebra software. In *Proceedings of the 1998 ACM/IEEE conference on Supercomputing*, pages 1–27. IEEE Computer Society, 1998.
- [51] R. C. Whaley, A. Petitet, and J. J. Dongarra. Automated empirical optimization of software and the atlas project. *PARALLEL COMPUTING*, 27:2001, 2000.
- [52] S. Wienke, P. Springer, C. Terboven, and D. an Mey. Openacc—first experiences with real-world applications. In *European Conference on Parallel Processing*, pages 859–870. Springer, 2012.
- [53] Z. Xianyi, W. Qian, and Z. Chothia. Openblas. URL: <http://xianyi.github.io/OpenBLAS>, 2014.
- [54] Y. Zhao, J. Li, C. Liao, and X. Shen. Poster: Bridging the gap between deep learning and sparse matrix format selection. In *Parallel Architectures and Compilation Techniques (PACT), 2017 26th International Conference on*, pages 152–153. IEEE, 2017.

Decision Tree Name	Accuracy (%)	DTPR	DTRR	Total number of Leaves	Decision Tree Height	Min Samples PerLeaf	Number of Unique Config. Gemm	Number of Unique Config. GemmDirect	Number of Leaves Gemm	Number of Leaves GemmDir
h1-L1	62	0.376	0.637	2	1	1	1	1	1	1
h1-L2	62	0.376	0.637	2	1	2	1	1	1	1
h1-L4	62	0.376	0.637	2	1	4	1	1	1	1
h1-L0.1	62	0.376	0.637	2	1	0.1	1	1	1	1
h1-L0.2	62	0.376	0.637	2	1	0.2	1	1	1	1
h1-L0.3	59	0.436	0.736	2	1	0.3	0	2	0	2
h1-L0.4	56	0.444	0.735	2	1	0.4	1	1	1	1
h1-L0.5	51.5	0.433	0.734	1	0	0.5	0	1	0	1
h2-L1	62	0.433	0.734	4	2	1	1	2	2	2
h2-L2	62	0.416	0.703	4	2	2	1	2	2	2
h2-L4	62	0.415	0.702	4	2	4	1	2	2	2
h2-L0.1	62	0.415	0.702	4	2	0.1	1	2	2	2
h2-L0.2	62	0.416	0.703	3	2	0.2	1	2	1	2
h2-L0.3	59	0.416	0.982	3	2	0.3	0	3	0	3
h2-L0.4	56	0.606	0.736	2	1	0.4	1	1	1	1
h2-L0.5	51.5	0.445	0.734	1	0	0.5	0	1	0	1
h4-L1	67	0.687	1.120	16	4	1	1	5	2	14
h4-L2	67	0.688	1.122	16	4	2	1	5	2	14
h4-L1	67	0.686	1.119	16	4	4	1	5	2	14
h4-L0.1	65.5	0.576	0.931	8	4	0.1	1	4	2	6
h4-L0.2	62	0.506	0.845	4	3	0.2	1	3	1	3
h4-L0.3	59	0.605	0.981	3	2	0.3	0	3	0	3
h4-L0.4	56	0.445	0.737	2	1	0.4	1	1	1	1
h4-L0.5	51.5	0.434	0.735	1	0	0.5	0	1	0	1
h8-L1	67	0.806	1.340	215	8	1	1	9	4	211
h8-L2	66.5	0.807	1.341	201	8	2	1	8	4	197
h8-L4	66	0.806	1.304	175	8	4	1	6	4	171
h8-L0.1	65.5	0.576	0.931	8	4	0.1	1	4	2	6
h8-L0.2	62	0.506	0.845	4	3	0.2	1	3	1	3
h8-L0.3	59	0.606	0.982	3	2	0.3	0	3	0	3
h8-L0.4	56	0.445	0.736	2	1	0.4	1	1	1	1
h8-L0.5	51.5	0.433	0.734	1	0	0.5	0	1	0	1
hMax-L1	60	0.852	1.424	1290	19	1	1	11	4	1286
hMax-L2	58.5	0.848	1.418	790	18	2	1	8	4	786
hMax-L4	64	0.846	1.412	430	15	4	1	6	4	426
hMax-L0.1	65.5	0.574	0.927	8	4	0.1	1	4	2	6
hMax-L0.2	62	0.506	0.844	4	3	0.2	1	3	1	3
hMax-L0.3	59	0.606	0.982	3	2	0.4	0	3	0	3
hMax-L0.4	56	0.445	0.737	2	1	0.4	1	1	1	1
hMax-L0.5	51.5	0.433	0.734	1	0	0.5	0	1	0	1

Table 5. Statistics of the decision trees trained from *go2* dataset by varying *H* and *L* on the Nvidia P100. The model with the highest **DTPR** score is reported in bold.

Decision Tree Name	Accuracy (%)	DTPR	DTRR	Total number of Leaves	Decision Tree Height	Min Samples PerLeaf	Number of Unique Config. Gemm	Number of Unique Config. GemmDirect	Number of Leaves Gemm	Number of Leaves GemmDir
h1-L1	55	0.692	1.085	2	1	1	0	2	0	2
h1-L2	55	0.560	0.828	2	1	2	0	2	0	2
h1-L4	55	0.600	0.895	2	1	4	0	2	0	2
h1-L0.1	55	0.702	1.092	2	1	0.1	0	2	0	2
h1-L0.2	55	0.631	0.955	2	1	0.2	0	2	0	2
h1-L0.3	42	0.619	0.918	2	1	0.3	0	1	0	2
h1-L0.4	42	0.559	0.822	2	1	0.4	0	1	0	2
h1-L0.5	42	0.418	0.691	2	1	0.5	0	2	0	2
h2-L1	52.5	0.638	1.012	4	2	1	0	2	0	4
h2-L2	52.5	0.544	0.823	4	2	2	0	2	0	4
h2-L4	52.5	0.500	0.749	4	2	4	0	2	0	4
h2-L0.1	55	0.572	0.863	4	2	0.1	0	2	0	4
h2-L0.2	55	0.540	0.820	3	2	0.2	0	2	0	3
h2-L0.3	42	0.555	0.831	2	1	0.3	0	1	0	2
h2-L0.4	42	0.560	0.838	2	1	0.4	0	1	0	2
h2-L0.5	42	0.499	0.715	2	1	0.5	0	2	0	2
h4-L1	56.5	0.641	1.005	16	4	1	1	2	1	15
h4-L2	58	0.517	0.781	16	4	2	1	2	0	15
h4-L1	56.5	0.677	1.062	15	4	4	1	2	0	14
h4-L0.1	55	0.577	0.878	7	4	0.1	0	4	0	7
h4-L0.2	55	0.446	0.681	4	3	0.2	0	3	0	4
h4-L0.3	42	0.502	0.742	2	1	0.3	0	1	0	2
h4-L0.4	42	0.529	0.778	2	1	0.4	0	1	0	2
h4-L0.5	42	0.440	0.617	2	1	0.5	0	2	0	2
h8-L1	55	0.584	0.863	84	8	1	5	13	6	78
h8-L2	56.5	0.466	0.669	60	8	2	2	9	3	57
h8-L4	52.5	0.551	0.826	45	8	4	1	7	2	43
h8-L0.1	55	0.473	0.682	8	5	0.1	0	5	0	8
h8-L0.2	55	0.466	0.669	4	3	0.2	0	3	0	4
h8-L0.3	42	0.571	0.850	2	1	0.3	0	1	0	2
h8-L0.4	42	0.592	0.885	2	1	0.4	0	1	0	2
h8-L0.5	42	0.591	0.865	2	1	0.5	0	2	0	2
hMax-L1	52.5	0.846	1.008	166	17	1	9	16	15	151
hMax-L2	54	0.570	0.858	95	15	2	3	12	4	91
hMax-L4	52.5	0.554	0.815	53	10	4	1	7	2	51
hMax-L0.1	55	0.487	0.708	8	5	0.1	0	5	0	8
hMax-L0.2	55	0.438	0.667	4	3	0.2	0	3	0	4
hMax-L0.3	42	0.628	0.954	2	1	0.3	0	1	0	2
hMax-L0.4	42	0.604	0.895	2	1	0.4	0	1	0	2
hMax-L0.5	42	0.496	0.714	2	1	0.5	0	2	0	2

Table 6. Statistics of the decision trees trained from *AntonNet* dataset by varying H and L on the ARM Mali-T860. The model with the highest **DTPR** score is reported in bold.